Salinity-Based Spatial Evaluation of Groundwater Quality for Agricultural Use

Parisa Pashahkhah
Islamic Azad University Science and Research Branch
Hossein Babazadeh (h_babazadeh@hotmail.com)
Islamic Azad University Science and Research Branch https://orcid.org/0000-0003-3838-5383
Shahram Shahmohammadi-Kalalagh
Islamic Azad University Tabriz Branch https://orcid.org/0000-0001-9131-8273
Mahdi Sarai-Tabrizi
Islamic Azad University Science and Research Branch https://orcid.org/0000-0002-4903-9307

Research Article

Keywords: Groundwater quality, Effective salinity, Potential salinity, Geostatistics, Semi-variogram, Miandoab Plain

Posted Date: September 24th, 2021

DOI: https://doi.org/10.21203/rs.3.rs-844577/v1

Version of Record: A version of this preprint was published at International Journal of Environmental Science and Technology on January 13th, 2022. See the published version at https://doi.org/10.1007/s13762-021-03881-3.

Salinity-Based Spatial Evaluation of Groundwater Quality for Agricultural Use

Abstract

The Miandoab Plain has the largest water reserve in the province of West Azerbaijan, northwest Iran. Groundwater resources along with surface-water meet the needs of urban, industrial, and agricultural sectors, and therefore, their quality should be examined. Water quality indices are useful tools for aquifer management. In this research, the groundwater quality of the Miandoab Plain for agricultural purposes was investigated. For this purpose, the concentrations of the ions Mg^{2+}, Ca^{2+}, Na^{+}, Hco_3^{-}, So_4^{2-}, Cl^{-} and the pH level were measured. The indices effective salinity and potential salinity as well as sodium adsorption ratio and electrical conductivity were analyzed to evaluate the salinity. The geostatistical analysis was performed using the GS^{+} software, and the zoning maps of salinity hazard were prepared using ArcGIS. To prepare the maps, EC, ES, PS, and SAR as well as Mg^{2+}, Ca^{2+}, Na^{+}, Hco_3^{-}, So_4^{2}, and Cl^{-} were selected based on the semi-variogram values and cross-validation technique. The Cl^{-} map was considered as the basis for preparing the groundwater quality maps of the region. The results showed that the groundwater quality in the east of the plain is suitable, in the central part can be recommended under constant supervision, and in the west is unsuitable for agriculture. In other words, according to the geography of the plain, the recharge area is the low-risk part of the plain and the salinity hazard increases toward the discharge area. The results can pave the way for the relevant organizations to plan for the agricultural and environmental sectors.

Keywords: Groundwater quality, Effective salinity, Potential salinity, Geostatistics, Semi-variogram, Miandoab Plain.

1. Introduction

Optimum use of groundwater requires proper management of exploitation which in turn needs scientific and principled knowledge of water resources in a region. Water quality indicators, as useful tools for water resources management, are usually intended for managers and decision-makers in a simple understandable way to transmit information on the quality and potential uses of a water body based on some criteria (Delgado et al., 2010). The Miandoab Plain is the main plain of Lake Urmia catchment and one of the agricultural hubs in the northwest of Iran. The turnover and economy of the plain is directly or indirectly dependent on the agricultural sector, most of the water needed for which is supplied from the groundwater resources. Almost half of the surface currents entering Lake Urmia pass through the Miandoab Plain, and 20 percent of the total groundwater abstraction in the catchment belongs to this plain. Therefore, proper management of the groundwater resources in the Miandoab Plain is necessary (Emami et al., 2018). Limited studies have been conducted on the groundwater of the Miandoab Plain: Emami et al. (2018) predicted the groundwater level of the Miandoab Plain using the artificial neural network (ANN), and the election (EA) and genetic (GA) algorithms. They concluded that the EA, with a root mean square error (RMSE) of 0.027, coefficient of correlation (R^2) of 0.93, and Nash-Sutcliffe efficiency coefficient (NSE) of 0.74, had a better performance in predicting the groundwater level than the ANN and GA. Jonubi et al. (2018) investigated the quantitative changes in the groundwater table of the Miandoab Plain using the MODFLOW-NWT model. The results showed that out of the water no longer pumped, respectively 34 and 41 mcm flow out of the downstream area toward Lake Urmia as underground stream. Also, respectively 40 and 51 mcm discharge into the surface-water resources, and the remains are stored in the plain. They stated that the continuation of this condition for five years would lead the middle lands of the plain to be swamped. The amount of agricultural return water flow in scenarios 1 and 2 were 28 and 20 percent, which showed a

decrease of 5 and 13 percent, respectively, compared to the present condition (33 percent). In scenario 3, the water-table dropped by 1.5 and 3 m after one and five years, respectively, but could supply 495 mcm of water for the reclamation of Lake Urmia during these five years. Noroozi-Qushbulaq et al. (2019) evaluated the vulnerability of the Miandoab Plain to nitrate using the GA. The optimized drastic (with the GA) had a higher correlation with nitrate, and therefore presented better results than the drastic model did. The optimized map showed that about 18, 11, 28, 26, and 17 percent of the plain are located in the very low, low, medium, high, and very high vulnerable areas, respectively.

Geostatistical method is one of the most accurate methods for estimating the values of variables at points where sampling has not been done. This method is based on the calculation of the weighted average of the values in the neighborhood of the estimation block. Geostatistical methods have widely been used in water engineering, some of which are as follows: Kresic (1997) introduced the Kriging method as the best and most powerful tool for data interpolation in the field of water resources and preparation of qualitative and quantitative zoning maps of groundwater parameters. Delgado et al. (2010), using the effective salinity and potential salinity, investigated the groundwater quality in Yucatan, Mexico. Ghariba et al. (2016) evaluated groundwater quality using GIS-based geostatistical algorithms. After analyzing the groundwater quality parameters, they created the maps of each parameter using the Kriging approach. The empirical semi-variogram values were tested for the Kriging models to find the best-fitted one on the basis of mean square error (MSE), root mean square error (RMSE), average standard error (ASE), and root mean square standardized error (RMSSE). The integrated method could sufficiently assess the environmental spatially-distributed parameters. Safiur Rahman et al. (2017) evaluated the water quality for sustainable agriculture in the district of Faridpur, Bangladesh. The irrigation water quality index showed that a large part of the samples was acceptable for irrigation. Other indices like sodium, sodium adsorption ration, residual sodium bicarbonate, total hardness, Kelley's ration, and magnesium adsorption ratio revealed similar results. The classification based on the Wilcox diagram and the permeability index led to similar outcome. The spatial mapping of the water quality index showed that the groundwater was more suitable for irrigation in the north of Faridpur than in the central and southern parts. Hamzah et al. (2017) emphasized the importance of the main hydro-geochemical characteristics and spatial distribution of the groundwater in Terengganu, Malaysia. Taheri Tizro and Mohamadi (2019) used a geostatistical approach to evaluate the groundwater quality in the Zarin Abad Plain, Iran. They concluded that the electrical conductivity ranged between 480 and 6580 $\mu S\ cm^{-1}$, and the major cations and anions were ranked as $Na^{+} > Ca^{2+} > Mg^{2+}$ and $So4^{2-} > Cl^{-} > Hco3-$. According to the values of RMSE and MAE, the Co-Kriging method was more optimum than the Kriging and inverse weighted distance strategies in evaluating the spatial variation of the groundwater quality parameters. Honarbakhsh et al. (2019) assessed the hydro-chemical quality of groundwater in semi-arid regions and mapped the qualitative parameters using ArcGIS. According to the Wilcox diagram, only 24% of the samples were in the C4-S4 class with high salinity and alkalinity. The maps showed that, due to the existence of dolomite and chalky formations in the south of the region, the groundwater in the north side was of better quality. Elkashouti (2019) studied the distribution of groundwater quality in the Nile Delta using geostatistical investigation (GIS) and concluded that the default Kriging was the best approach to map the hydro-geochemical parameters. Elubid et al. (2019) investigated the geospatial distribution of groundwater quality in the state of Gedaref, Sudan, using the GIS and drinking water quality index. The data used in the study comprised the samples of major cations and anions from forty wells. The results revealed that the groundwater quality was mainly controlled by the sodium and bicarbonate ions which defined the composition of the water type to be Na HCO3. Maroufpoor et al. (2019) examined the geostatistic-based Kriging and Co-Kriging methods

and compared the results with those of the ANN and ANFIS models in predicting the spatial distribution of groundwater quality in Kerman, Iran. Verma et al. (2020) used the water quality index and geographic information to analyze the groundwater quality in the district of Bokaro, India. The results indicated the slightly acidic to slightly alkaline nature of the groundwater. The concentrations of TDS, TH, Ca^{2+}, Mg^{2+}, $HCO3^{-}$, F^{-}, and $NO3^{-}$ exceeded the desirable and acceptable limits of the drinking water quality standards recommended by the Indian Standard Drinking Water Specification and the World Health Organization during the pre- and post-monsoon seasons, respectively. However, the concentrations of Na^{+}, K^{+}, Cl^{-}, and $SO4^{2-}$ were within the acceptable limits during both the seasons. The GIS maps displayed the low quality of the groundwater in the pre-monsoon season in comparison with the post-monsoon season. Jeon et al. (2020) studied the trend of temporal variations in the groundwater quality in the Key sectors of Korea. To analysis the sustainability of the drinking water, they compared the results with the guidelines developed by the World Health Organization (WHO) and the Korean Ministry of Environment (KME). For irrigation sustainability assessment, they used the US salinity laboratory (USSL), Wilcox diagram, electrical conductivity, sodium adsorption ration, sodium percent, and residual sodium carbonate. According to the WHO and KME, about 96% and 93% of the groundwater samples, respectively, were suitable for drinking. Based on the USSL and Wilcox diagram, about 98% and 83% of the samples were within the acceptable range for irrigation.

To our knowledge, despite the importance of quantity and quality of groundwater resources in the Miandoab Plain, there are a limited number of studies focusing on the distribution of groundwater quality in the plain from an agricultural perspective. On the other hand, no spatial analysis has yet been done on the groundwater resources in the plain, even though it can lead to better utilization of the resources and decrease in the soil destruction hazard. The aim of the present study is to analyze and assess the groundwater quality in the Miandoab Plain for agricultural uses based on geostatistical validation of major ions and salinity indices.

2. Materials and Methods

2.1. The Study Area

The alluvial aquifer of the Miandoab (Ghosha-Chay) Plain, as the fourth-most fertile plain in Iran, is the largest aquifer of Lake Urmia catchment. The plain is located inside the catchment in north-west Iran at longitude $36^{\circ}\ 50'$ to $37^{\circ}\ 15'$ east and latitude $45^{\circ}\ 50'$ to $46^{\circ}\ 15'$ north (Fig. 1). The aquifer is recharged from the north-east (the Mordaq-Chay River), east (the Lilan-Chay River), south-east (the Zarineh-Rood River), and south (the Simineh-Rood River) and discharged into the north-west (Lilan-Chay) and west (Zarineh-Rood and Simineh-Rood) of the plain. The Mordaq-Chay and Qoori-Chay rivers enter the plain from the north-east and east sides and immediately join the Lilan-Chay and Zarineh-Rood rivers. The Miandoab Plain has an area of 1256 km^2 and an average slope of 0.004. The plain is lowland in its entire area and is a part of the Alborz-Azerbaijan structural tectonic zone. The Zarineh irrigation and drainage network with an area of 586 km^2 is located in the plain. The Miandoab study area is divided into two main areas in terms of accessibility to the irrigation and drainage network: The areas located in the Miandoab network including Z_1, Z_2, Z_3, Z_4, Z_5, Z_6, Z_7, Z_8, $Z_{9\text{-}1}$, $Z_{9\text{-}2}$, $Z_{9\text{-}3}$, $Z_{9\text{-}4}$, $Z_{9\text{-}5}$ and the areas outside of the network including M_1, M_2, L_1, L_2, G, S, ZN, ZP. Therefore, the plain consists of the areas located in the Miandoab network and all the farmlands in L_2, G, S, ZN and and ZP (Jonubi et al., 2018).

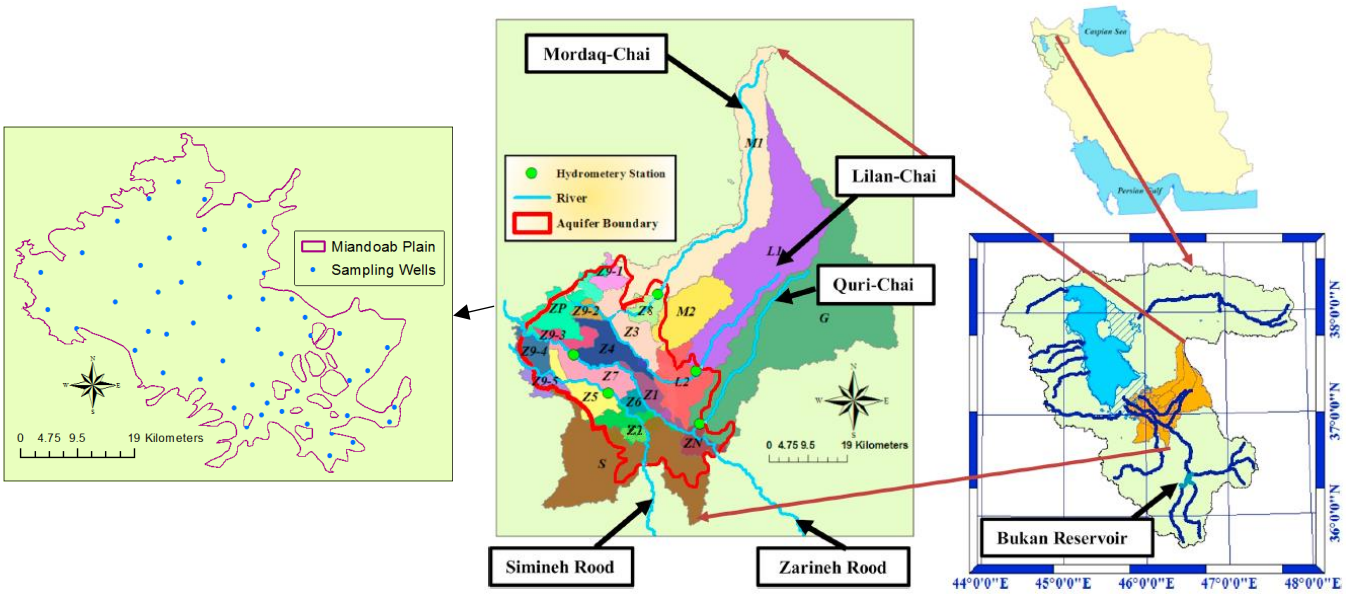

Fig. 1. The geographical location of the study area and sampling wells.

The topography of the plain is uniform and smooth with only a few small hills in the central part. The plain is at an average elevation of 1292 m, with the lowest and highest points at the elevations of 1297 and 1400 m, respectively. The region has different geological formations. However, alluvial formations form the main part of the plain, which has emerged in the form of alluvial fans and fluvial deposits. The thickness of the alluvium varies across the plain, ranging from a few meters in the vicinity of the surrounding mountains to more than 150 m near the cities of Miandoab and Malekan. In the north of the plain, on the bed of the Mordaq-Chay River, the thickness of the alluvial deposits reaches up to 80 m. In the east, the thickness is about 30 m with thin layers of clay, but it even reaches up to 160 m due to the presence of the Lilan-Chay River (Emami et al., 2018).

Based on the Emberger's empirical climagram and using the data from the Miandoab synoptic station, the region has a cold semi-arid climate. As the aquifer is recharged by precipitation, the climate of the region is of great importance. The amount of precipitation in the region increases from the plain toward the heights. According to the thirty-year data set of 1988-2017, the average annual precipitation in the Miandoab study area is about 284 mm year^{-1}. The amount of potential evapotraspiration and pan evaporation are 742 and 1650 mm year^{-1}, respectively (Noroozi-Qushbulaq et al., 2019). According to the latest statistics, the amount of groundwater abstraction through 14096 wells in the study area is equal to 350 MCM year^{-1}, 240 MCM of which belongs to the aquifer of the Miandoab Plain (Emami et al., 2018).

2.2. Method

To investigate the spatial and temporal variations of the groundwater quality parameters in the Miandoab Plain, the data set of 2002-2018 collected from 51 wells of the monitoring network by the Regional Water Company of West Azerbaijan was used. The data had been recorded in the form of laboratory results, solutes and necessary parameters including cations and anions. The emphasis was on the three cations sodium, calcium, and magnesium, and the four anions chlorine, sulfate, carbonate, and bicarbonate since these ions are more abundant than the other solutes in water. The long-term trend of the parameters are shown in Fig. 2.

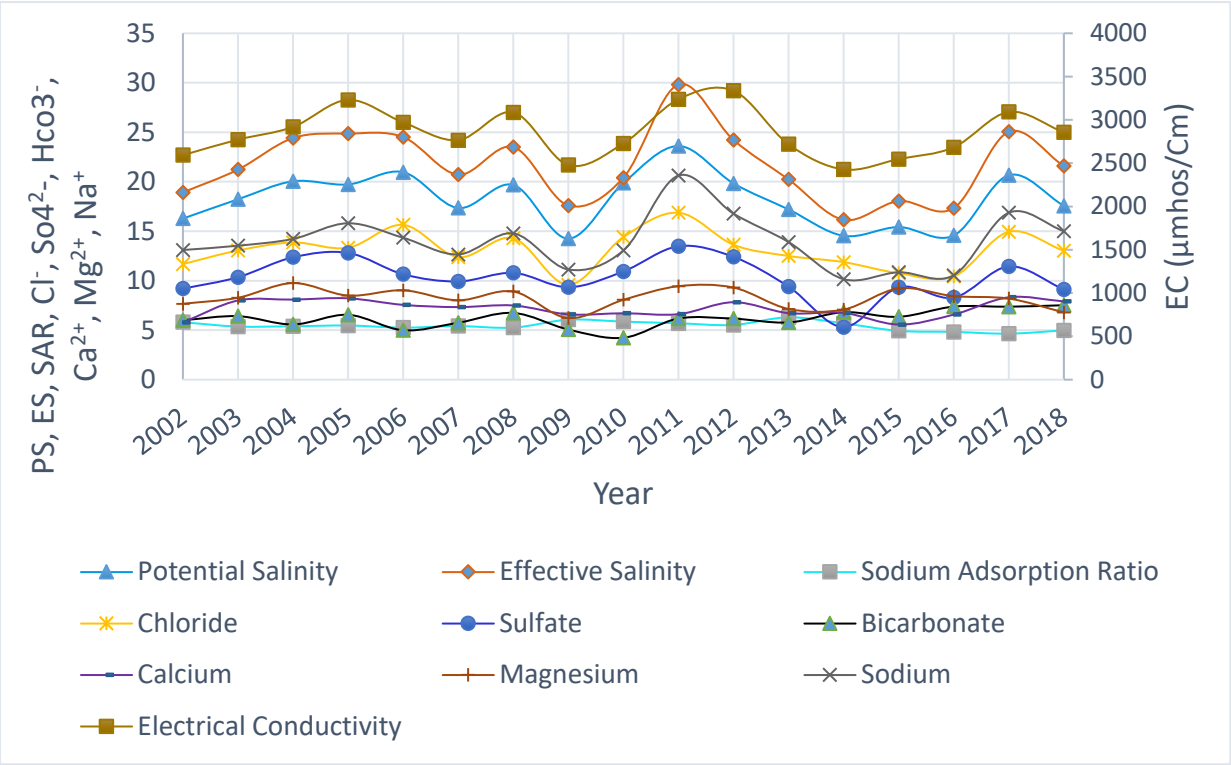

Fig. 2. Temporal variations of the groundwater quality parameters in the Miandoab Plain

First all the parameters were normalized and then the classical statistical analysis was performed using the Kolmogorov-Smirnov test at a significance level of 5% in the SPSS22 software. If the data distribution did not follow the normal distribution, the logarithmic transformation was used. The Excel software was used to examine the presence or absence of a trend in the data. The empirical semi-variogram of the qualitative data was calculated using the GS^+ software and the best model was selected for each parameter. The interpolations were performed using the Kriging and inverse distance weighting methods. The interpolation methods were evaluated and validated using the cross-validation technique. To determine the best interpolation method for mapping the qualitative parameters, RMSE and ME as error criteria, and r as correlation coefficient were used; the method with the lowest RMSE and ME, and highest r was selected as the most appropriate one. Finally, using the ArcGIS software, the zoning maps of the groundwater salinity hazard were prepared.

2.3. The Groundwater Quality for Agriculture

Salinity is one of the most important indices in evaluating groundwater quality. One of the techniques for determining salinity is to measure electrical conductivity; the higher the amount of solutes in the water is, the higher the electrical conductivity is. The increase in salinity reduces the osmotic activity of plants and, as a result, the adsorption of water and nutrients from the soil (Saleh et al. 1999). Each crop, depending on its type, can tolerate salinity up to a threshold level above which the yields decrease per unit of increase in salinity (Maas and Hoffman, 1977; Maas and Grattan, 1999). In case of high salinity, some new indices such as effective salinity and potential salinity have been introduced (Delgado et al., 2010). Sodium adsorption ratio is also a suitable index to evaluate soil alkalinity hazard (Subramani et al., 2005; Kaur et al., 2017). There can also be chloride toxicity hazard in groundwater (Richards, 1954). Hence, the electrical conductivity (EC), effective salinity (ES), potential salinity (PS),

sodium adsorption ratio (SAR), and the ions affecting these indices, i.e. Mg^{2+}, Ca^{2+}, Na^{+}, Hco_3^{-}, So_4^{2-} and Cl^{-} were chosen in the present study.

The Wilcox classification, also known as the US salinity laboratory method (Rafi Sharifabad et al., 2017), was used to determine the agricultural water quality. According to this classification and the values of EC and SAR, the agricultural water quality is classified into four categories: excellent, good, medium, and not recommended (Table 1), and 16 classes (Table 2).

Table 1. The classification of agricultural water quality (Wilcox, 1995).

Water quality	EC (µmhos Cm^{-1})	Category EC	SAR $(mmol\ L^{-1})^{0.5}$	Category SAR
E	<250	C_1	<10	S_1
G	250-750	C_2	10-18	S_2
M	750-2250	C_3	18-26	S_3
NR	>2250	C_4	>26	S_4

E= Excellent; G= Good; M= Medium; N= Not Recommended.

Table 2. The different classes of water quality according to the Wilcox classification (Wilcox, 1995).

-	Agricultural water quality	Category Water
1	fresh, completely safe for agriculture	C_1S_1
2	slightly saline, almost suitable for agriculture	C_2S_1, C_2S_2, C_1S_2
3	saline, usable for agriculture after the necessary preparations	C_3S_3, C_3S_2, C_3S_1, C_2S_3, C_1S_3
4	highly saline, hazardous to agriculture	C_4S_1, C_4S_2, C_4S_3, C_4S_4, C_3S_4, C_2S_4, C_1S_4

Sodium adsorption ratio [$(mmol\ L^{-1})^{0.5}$] is defined as sodium concentration ($mmol\ L^{-1}$) relative to calcium and magnesium concentrations ($mmol\ L^{-1}$).

In the SAR classification (Fig. 3), S_1 can be used for majority of soils which are less capable of reaching high exchangeable sodium content. S_2 can cause problems in fine-textured soils which do not contain gypsum and have a high cation exchange capacity, as well as when leaching is not possible. S_3 can cause the toxicity due to exchangeable sodium in irrigated soils; hence proper drainage, double leaching, and addition of organic matter would be necessary (however in soils containing large amounts of gypsum, there are less hazard). S_4; the soil is not suitable for irrigation, except in low or medium salinity conditions or when using gypsum as soil conditioner (Richards, 1954; Delgado et al, 2010).

$$SAR = \frac{Na^{+}}{\sqrt{(Mg^{2+} + Ca^{2+})/2}} \quad (1)$$

Electrical conductivity is an indirect measurement of the total concentration of salts dissolved in water, presented at the temperature of 25 °C.

In the EC classification (Fig. 3), C_1 can be used for a large number of crops and soils with low salinity hazard. C_2 can be applied to crops which are able to tolerate medium salinity. C_3 cannot be used for soils with poor drainage. Therefore, it is necessary to choose crops which are significantly tolerant of salinity, even when drainage is in good condition. C_4 is not usually suitable for irrigation, but if necessary, can be used for crops cultivated in highly permeable well-drained soils (Richards, 1954; Palacios and Aceves, 1970; Ayers and Wescott, 1994; Delgado et al, 2010).

For the EC values greater than 250 µmhos cm^{-1}, ES and PS were also used since some salts can precipitate and in some others the relative concentration can increase due to evaporation (Palacios and Aceves, 1970; Delgado et al., 2010).

Potential salinity is the estimation of risk of high salt concentrations due to the presence of Cl^{-} and SO_4^{2}, which can increase the osmotic potential of the soil solution when the available soil moisture content is less than 50%. The classification of water quality in terms of salinity

based on the PS values is presented in Table 3. This index is defined as follows (Delgado et al., 2010):

$$PS = Cl^{-} + (^{1}/_{2})SO_4^{2-} \quad (2)$$

Effective salinity is another index developed to consider relative solubility of various salts that are likely to exist in water. ES provides a more precise estimate of risk of osmotic pressure increase in soil solution when carbonate and bicarbonate concentrations are high (Kirda, 1997). Under this condition, the calcium and magnesium carbonates and calcium sulfate precipitate, thus preventing an increase in the osmotic pressure in the solution. Water quality in terms of salinity based on ES is the same as the PS classification (Table 3). This index is described as follows (Delgado et al., 2010):

If $Ca^{2+} > (CO_3^{2-} + HCO_3^{-} + SO_4^{2-})$
$Then: ES = (\sum cations\ or\ \sum anions) - (CO_3^{2-} + HCO_3^{-} + SO_4^{2-})$ (3)

If $Ca^{2+} < (CO_3^{2-} + HCO_3^{-} + SO_4^{2-})$, but $Ca^{2+} > (CO_3^{2-} + HCO_3^{-})$
$Then: ES =$ (4)
$(\sum cations\ or\ \sum anions) - (Ca^{2+})$

If $Ca^{2+} < (CO_3^{2-} + HCO_3^{-})$, but $(Ca^{2+} + Mg^{2+}) > (CO_3^{2-} + HCO_3^{-})$
$Then: ES = (\sum cations\ or\ \sum anions) - (CO_3^{2-} +$ (5)
$HCO_3^{-})$

If $(Ca^{2+} + Mg^{2+}) < (CO_3^{2-} + HCO_3^{-})$
$Then: ES = (\sum cations\ or\ \sum anions) -$ (6)
$(Ca^{2+} + Mg^{2+})$

where, the sum of cations or the sum of anions means the use of the highest value (Palacios and Aceves, 1970; Delgado et al, 2010).

Table 3. Water quality in terms of salinity based on the values of ES and PS (Delgado et al, 2010).

Water quality	PS and ES (mmol L^{-1})
G	< 3
M	3 - 15
NR	> 15

G= Good; M= Medium; NR= Not Recommended.

Chlorides and some other ions, even in small amounts, can sometimes be toxic elements to plants and fruit trees. Water toxicity based on chloride, bicarbonate and sodium is presented in Table 4 (Ayers and Wescott, 1994; Delgado et al, 2010).

Table 4. Water toxicity based on Chloride, Bicarbonate and Sodium.

Water toxicity	Cl^{-} (mmol L^{-1})	Hco_3^{-} (mmol L^{-1})	Na^{+} (mmol L^{-1})
WR	< 4	< 1.5	< 9.5
S - M	4 - 9	1.5 - 7.5	= 9.5
S	> 9	> 7.5	> 9.5

WR= Without Restriction; S–M= Slight to Moderate; S= Severe.

2.4. Geostatistical Analysis

Geostatistics is a subdiscipline of applied statistics that using information obtained from observed points provides a wide range of statistical estimators in order to estimate the desired characteristic at unobserved points. One of the tools for geostatistical studies is a function

called variogram which allows the analysis of scale structure and intensity of spatial variation of regional variables. The GS^+ software is a comprehensive program which provides all geostatistical components including variogram analysis as well as mapping in an integrated and flexible way. Among the most important features of this software, which have also been used in the present study, are:

(1) Spatial autocorrelation analysis: the semi-variogram analysis, which is used to examine the spatial correlation between observed data; it is assumed that the points close to each other have similar values. Drawing isotropic and anisotropic variograms is another capability of this part.

(2) Interpolation: (a) Kriging (Point Kriging, Block Kriging, and Co-Kriging); optimum interpolation based on spatial correlation, (b) inverse distance weighting and normal distance weighting for analyzing the nearest neighbor, and (c) the output compatible with mapping programs such as ArcGIS.

(3) Calculation of statistical parameters: (a) mean and variance of the sample, (b) skewness and kurtosis, (c) frequency distribution (normal probability plots, cumulative frequency plots, and frequency histograms), (d) data normalization transformations, (e) quantile scattergrams (indicating the values of sampling points throughout the spatial domain), and (f) regression analysis (Khosravi and Abbasi, 2015).

In geostatistics, to study the structure of the variability of the studied variable with respect to distance (spatial or temporal), it is necessary to establish an appropriate semi-variogram function. For this purpose, the sum of the squares of the difference between the point pairs that are at a known distance of h from each other should be calculated and drawn versus h (Sanches, 2001). Thus, semi-variogram is a distance-dependent variance denoted by γ. The semi-variogram γ (h) for n sample pairs $Z(x_i)$ and $Z(x_i+h)$, at a distance of h from each other, can be calculated as follows (Isaaks and Srivastava, 1989; Hernandez-Stefanoni and Ponce-Hernandez, 2006; Delgado et al, 2010):

$$\gamma(h) = \frac{1}{2n}\sum_{i=1}^{n}[Z(x_i) - Z(x_i + h)]^2 \quad (7)$$

where, $Z(x_i)$ and $Z(x_i+h)$ represent the values of water quality at the point i and the other points isolated from X_i at a distance of h, respectively.

Each semi-variogram has three main characteristics: (1) nugget effect (C_0); the variogram value at the origin of the coordinate system (h=0). The closer the nugget effect is to zero, the more optimum the model is. (2) sill (C_o+C): as the distance increases, the semi-variogram value increases and tends to a constant limit called the sill. In the Kriging method, the variograms with a certain sill are more important. (3) range of influence: the spatial distances between the samples beyond which the regional variables at adjacent points have no significant effects on each other. The larger the range of influence is, the wider the spatial structure is, and therefore the range from which the data can be obtained to estimate unknown values enlarges. The range of influence is widely used in analyzing structural anisotropy and designing optimum distances in sampling networks (Shabani et al, 2009).

Since the number of samples used in this study was 51, the isotropic semi-variogram was selected as the most suitable semi-variogram, because anisotropic semi-variograms require more samples. Among the common models, the one with a higher coefficient of determination (r^2), and lower nugget effect (C_0) and residual sum of squares (RSS) was selected as the best model to show the variogram (Isaaks and Srivastava, 1989; Webster and Oliver, 1990; Delgado et al, 2010).

The data were estimated using the Kriging and inverse distance weighting interpolation methods as follows:

1) Kriging is the most common geostatistical method. This method is an estimation technique based

on weighted moving average and is known as the best linear unbiased estimator (Ghasemi-Ziarani et al., 2006). The use of the Kriging method is valid if the variable Z has a normal distribution. Otherwise, the nonlinear Kriging method should be used or the variable distribution should be normalized (Rafi Sharif Abad et al., 2017). Kriging is generally described as (Delgado et al., 2010):

$$Z(x_0) = \sum_{i=1}^{n} \lambda_i Z(x_i) \quad (8)$$

where, $Z(x_0)$ is the optimum estimate of water quality, λ_i is the optimum weight chosen to minimize the estimation variance of the sample i, $Z(x_i)$ is the observed water quality, and n is the number of observed data.

2) Inverse distance weighting is another geostatistcal method which obtains the unknown quantity by

weighting the data adjacent to a point and performs the interpolation. It is assumed that points close to each other are more similar than the farther points, and therefore closer points have more weight. Inverse distance weighting is obtained using Eq. 9:

$$Z = \frac{1/d_i^p}{\sum_{i=1}^{n} 1/d_i^p} \quad (9)$$

where, d_i is the distance between x_0 and x_i, p is the power of the parameter, and n is the total number of samples (Rafi Sharif Abad et al., 2017).

The main difference between the above-mentioned interpolation methods is that the inverse distance weighting is a classical statistical method in which interpolation is based on the weight of points but Kriging is a geostatistical method expressing that in addition to the distance, the covariance of the data is also important.

There are different criteria for data validation, evaluation of the accuracy of the estimates and errors, and choosing the best interpolation method. In the present study, the cross-validation technique, mean error (ME), root mean square error (RMSE), and coefficient of correlation (r) were used to compare the observed and estimated values of the agricultural water quality (Hernandez-Stefanoni and Ponce-Hernandez, 2006; Delgado et al., 2010).

The cross-validation technique is one of the most important and common techniques for data validation. In this method, one observation point is removed at each stage and then is estimated using the remaining observation points. This is repeated for all the observation points, so that at the end there will be an estimate for each observation point and finally, having the observed and estimated values, errors and deviations can be determined (Bagheri and Mohammadi, 2009).

The mean error is used to determine the bias in the estimations according to Eq. 10 (Delgado et al., 2010):

$$ME = \frac{1}{n} \sum_{i=1}^{n} \overline{Z}(x_i) - Z(x_i) \quad (10)$$

where, n is the total number of samples, and $\overline{Z}(x_i)$ and $Z(x_i)$ are the estimated and observed values of water quality, respectively.

The root mean square error is a repeated measurement of the differences between the values estimated by a model and the observed values (Delgado et al., 2010). RMSE is a good criterion of accuracy and is used as an important parameter to show the precision of spatial analysis in ArcGIS (Nazarizadeh et al., 2006: Rafi Sharif Abad et al., 2017). This criterion is calculated using Eq. 11 (Delgado et al., 2010):

$$RMSE = \sqrt{\frac{\sum_{i=1}^{n}[\overline{Z}(x_i) - Z(x_i)]^2}{n}} \quad (11)$$

where, n is the total number of samples, and $\overline{Z}(x_i)$ and $Z(x_i)$ are respectively the estimated and observed values of water quality.

The coefficient of correlation is a criterion of the relation between two variables and is denoted by r. The value of r varies between -1 and +1 (Delgado et al., 2010).

This computation process is a comprehensive method for selecting the best ions and salinity indices in order to prepare zoning maps of spatial changes in groundwater quality for agricultural use (Delgado et al., 2010; Garbia et al., 2016).

3. Results and Discussion

3.1. Chemical Characterization of Samples

To analyze the suitability of groundwater in the region for agriculture, the data set of 2002-2018 was classified using the Wilcox diagram. The results are presented in terms of frequency in Table 5. According to Table 5, saline water has the highest frequency, but fresh water and slightly saline water have no frequency during the period. Highly saline water has occurred in 37% of the cases.

Table 5. The frequency of different groundwater classes in terms of agriculture according to the Wilcox diagram.

-	Agricultural water quality	Frequency
1	fresh, completely safe for agriculture	0%
2	slightly saline, almost suitable for agriculture	0%
3	saline, usable for agriculture after the necessary preparations	63%
4	highly saline, hazardous to agriculture	37%

Fig. 3 shows the Wilcox diagram of the aquifer over the study years. This diagram shows that the highest frequency belongs to the saline category. As shown in the zoning maps, salinity is much higher in the west of the plain (Figs. 6 and 7).

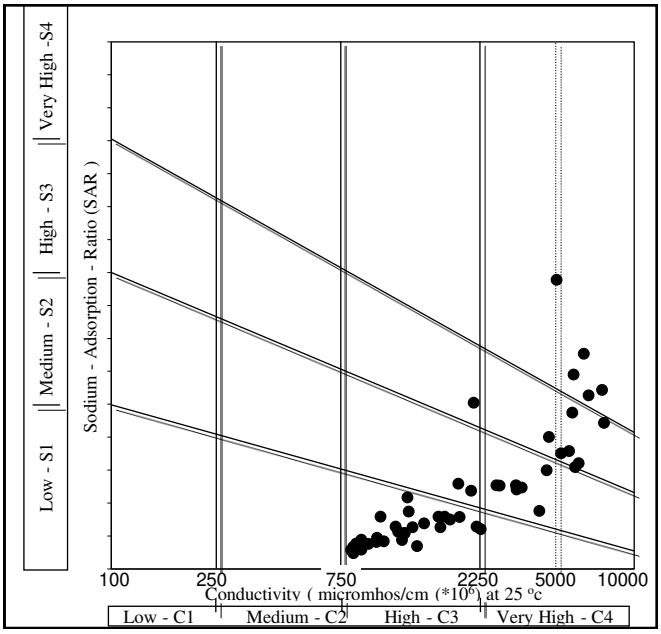

Fig. 3. The groundwater quality of the Miandoab Plain based on the hazards of sodicity and salinity.

The chloride concentration in 19 water samples (approximately 37% of the area of the plain) is less than 4 mmol L^{-1}, which has no restriction for agricultural use. The chloride concentration in 10 water samples (20% of the area) ranges from 4 to 9 mmol L^{-1} (low to moderate restriction). Finally, 22 samples (43% of the area) have a chloride concentration of more than 9 mmol L^{-1} (severe restriction).

The sodium content is less than 9.5 mmol L^{-1} (no restriction) in 25 water samples (49% of the total area) and more than 9.5 mmol L^{-1} (severe restriction) in 26 samples (51% of the area). However, no sodium percentage was found to fall into the low to moderate restriction category.

The bicarbonate concentration is 1.5-7.5 mmol L^{-1} (low to moderate restriction) in 40 samples (78% of the area) and more than 7.5 mmol L^{-1} (severe restriction) in 11 samples (22% of the area). Yet there is no bicarbonate percentage in the "no restriction" category.

Table 6. The descriptive statistics of ions, EC and groundwater quality indices.

Parameter	Unit	Valid N	Mean	Median	Min	Max	Std.Dev.	Skewness	Kurtosis
EC	µmhos Cm^{-1}	51	7.70	7.59	6.72	8.95	0.72	0.26	-1.33
SAR	$(mmol\ L^{-1})^{0.5}$	51	1.61	1.50	0.29	3.22	0.73	0.23	-0.85
ES	mmol L^{-1}	51	2.56	2.36	1.32	4.15	0.89	0.35	-1.24
PS	mmol L^{-1}	51	2.19	2.02	0.62	4.07	1.08	0.31	-1.20
Ca^{2+}	mmol L^{-1}	51	1.11	0.96	0.26	2.49	0.57	0.50	-0.82
Mg^{2+}	mmol L^{-1}	51	1.22	1.08	0.22	2.42	0.64	0.17	-1.41
Na^{+}	mmol L^{-1}	51	2.20	2.04	0.59	3.83	0.96	0.15	-1.19
Cl^{-}	mmol L^{-1}	51	1.87	1.55	0.10	4.00	1.20	0.38	-1.15
So_4^{2-}	mmol L^{-1}	51	1.41	1.44	0.00	2.62	0.72	-0.18	-1.26
Hco_3^{-}	mmol L^{-1}	51	1.77	1.70	1.25	2.69	0.32	0.68	0.29

The ions and salinity indices were analyzed using classical statistics and assessed (Table 6). According to Table 6, the standard deviation is more than 1 for PS and Cl^{-} and less than 1 for the indices EC, ES, SAR and other ions. All the standard deviation values are less than 2. In scientific studies, the data with a standard deviation of more than 2 from the mean value are usually considered as outliers and are excluded from analysis. Skewness and kurtosis are also used to test the normality of the data; if the values of both criteria are not in the range of -2 to 2, the data do not have a normal distribution (Habibi, 2016). The values of skewness and kurtosis were found to be in the ranges of -0.18 to 0.68 and -1.41 to 0.29, respectively, indicating the normal and symmetric distribution.

3.2. Spatial Analysis

According to Tables 7 and 8, the nugget variance, structural variance, ME, RMSE, r^2, and r were used to evaluate the estimated values.

Table 7. The characteristics of the semi-variogram models.

Ions,EC and Indexes	Unit	Model	Model r^2	Nugget Variance	RSS	Relative Structural Variance (%)
EC	µmhos Cm^{-1}	Gaussian	0.98	0.26	0.01	89.8
ES	mmol L^{-1}	Gaussian	0.98	0.34	0.01	87.3
PS	mmol L^{-1}	Gaussian	0.98	0.53	0.04	82.7
Na^{+}	mmol L^{-1}	Gaussian	0.98	0.43	0.02	85.5
Cl^{-}	mmol L^{-1}	Gaussian	0.97	0.56	0.10	82.1
Mg^{2+}	mmol L^{-1}	Gaussian	0.96	0.28	0.00	86.1
SAR	$(mmol\ L^{-1})^{0.5}$	Linear to sill	0.94	0.18	0.02	88.0
Hco_3^{-}	mmol L^{-1}	Gaussian	0.93	0.02	0.00	85.5
Ca^{2+}	mmol L^{-1}	Gaussian	0.89	0.24	0.00	83.2
So_4^{2-}	mmol L^{-1}	Gaussian	0.50	0.46	0.01	59.4

The concentrations of all the ions using the Gaussian semi-variogram with an r^2 of 0.5-0.98 are presented in Table 7 (Fig. 4). The parameter $[C/(C_o+C)]\times100$ indicates the ratio of structural variance to non-structural variance and determines what percentage of the data are structured; the more it tends to 1, the more structured the data become. The calculated structural variance is between 59.4 and 86.1%, suggesting a high spatial correlation of all the ions studied in the region. The values of nugget variance are small compared to those of structural variance, which also implies the identification of the spatial distribution pattern for these ions (Delgado et al., 2010).

The indices ES, PS, and EC were explained by the Gaussian model with an r^2 of 0.98, and SAR was explained by the linear to sill model with an r^2 of 0.94 (Fig. 5). The values of structural variance and nugget variance are 82.7-89.8% and 18-53.1%, respectively (Table 7). Accordingly, the spatial autocorrelation in the agricultural water quality indices was clearly identified by determining the Gaussian and linear models appropriate to the empirical semi-variograms (Fig. 5).

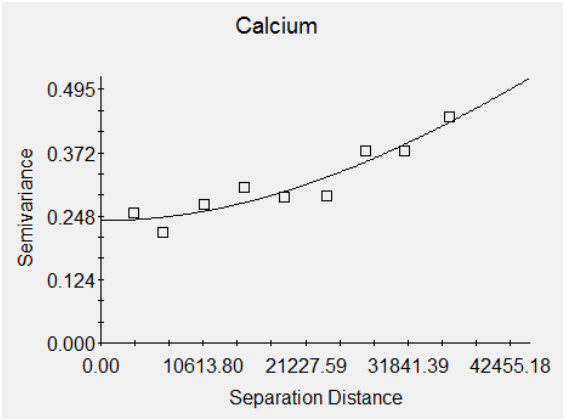

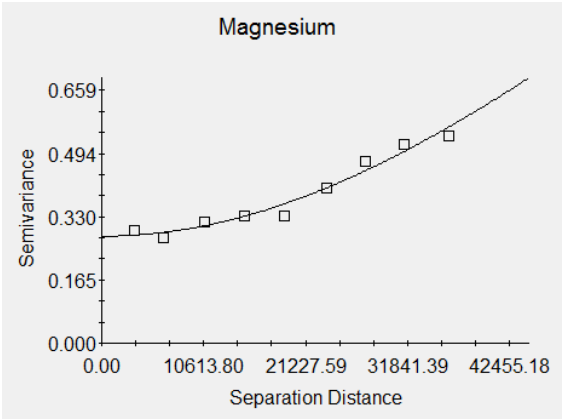

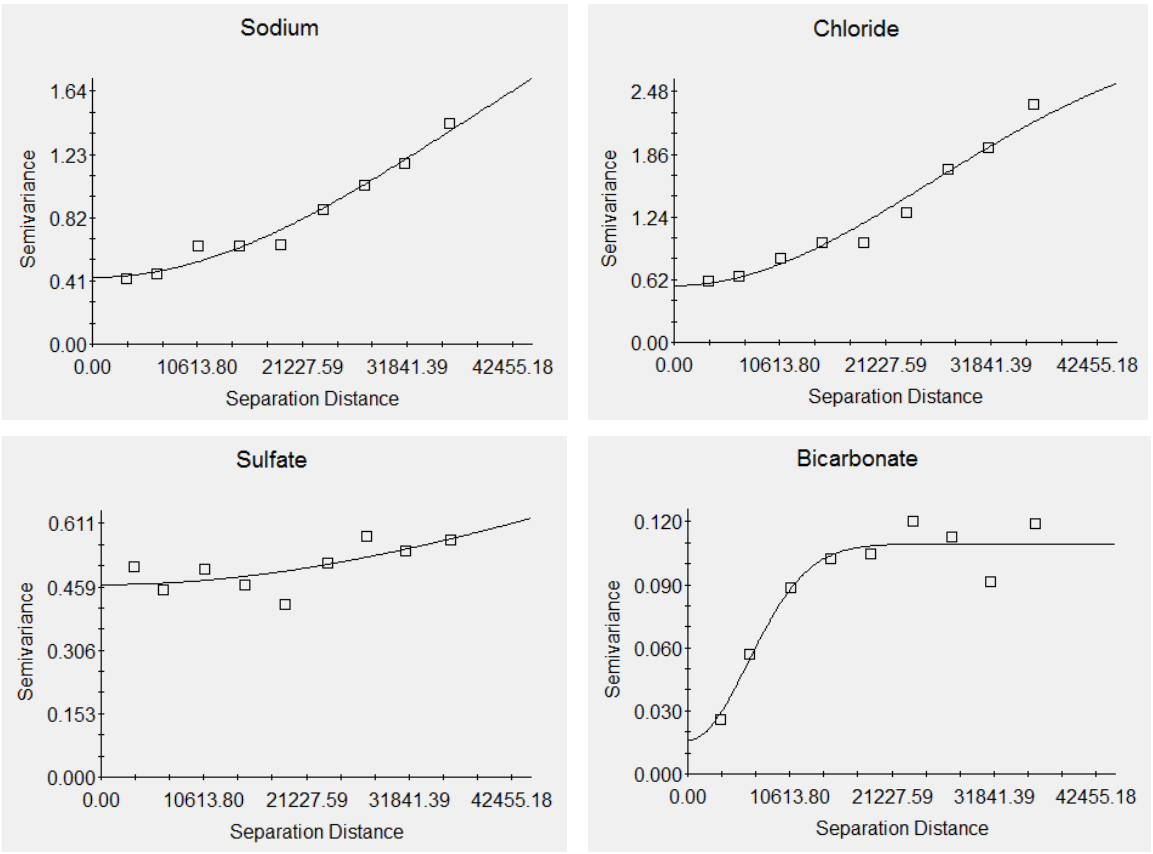

Fig. 4. The empirical semi-variograms for Calcium, Magnesium, Sodium, Chloride, Sulfate and Bicarbonate in the groundwater.

The cross-validation of the interpolations for the ions showed that r, ME, and RMSE of the observed and estimated values range between 0.22 and 0.71, 0.18 and 0.66, and 0.22 and 0.84, respectively. For EC, PS, ES, and SAR, these criteria are in the range of 0.62 to 0.67, 0.43 to 0.65, and 0.54 to 0.81, respectively (Table 8).

Table 8. The statistics of the cross-validation between the observed and estimated values for the water quality parameters.

Parameters	Unit	Interpolate	r	ME	RMSE
Cl^-	mmol L^{-1}	Kriging- Point Krig	0.71	0.66	0.84
Hco_3^-	mmol L^{-1}	Inverse Distance Weighting (IDW)	0.70	0.18	0.22
ES	mmol L^{-1}	Kriging- Point Krig	0.67	0.54	0.65
SAR	$(mmol\ L^{-1})^{0.5}$	Inverse Distance Weighting (IDW)	0.67	0.43	0.54
Na^+	mmol L^{-1}	Kriging- Point Krig	0.66	0.58	0.71
PS	mmol L^{-1}	Kriging- Point Krig	0.66	0.65	0.81
EC	µmhos Cm^{-1}	Kriging- Point Krig	0.62	0.45	0.56
Ca^{2+}	mmol L^{-1}	Kriging- Point Krig	0.49	0.40	0.50
Mg^{2+}	mmol L^{-1}	Kriging- Point Krig	0.45	0.47	0.57
So_4^{2-}	mmol L^{-1}	Kriging- Point Krig	0.22	0.58	0.71

In all the parameters, the ME and RMSE values indicated that the errors in the interpolation models are small, and therefore acceptable. The correlation coefficient of Cl^- is high and Hco_3^-, ES, SAR, Na^+, PS, and EC have good correlation coefficients, respectively, so were selected as criteria for preparing the groundwater salinity zoning maps of the Miandoab Plain. However, no map was prepared for Ca^{2+}, Mg^{2+}, and So_4^{2-} as they have correlation coefficients of less than 0.49 (Figs. 6 and 7).

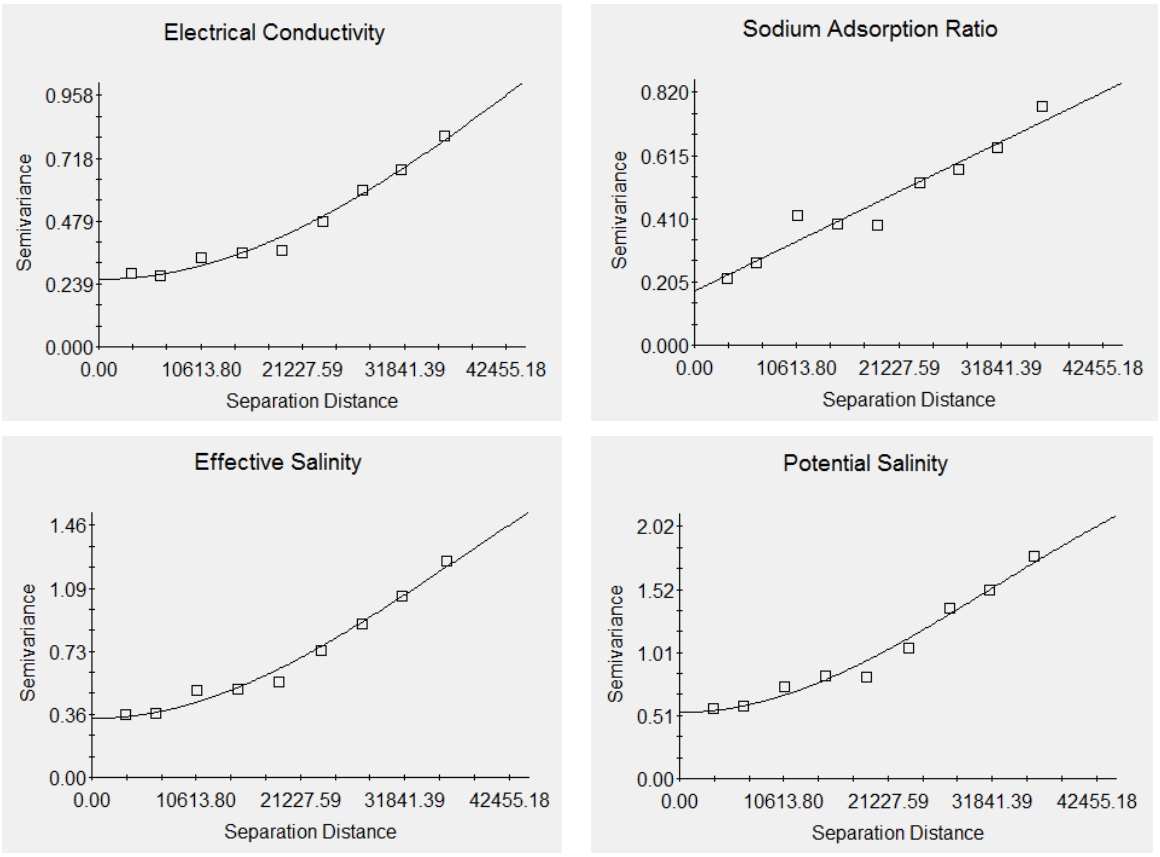

Fig. 5. The empirical semi-variograms for the Electrical Conductivity, Sodium Adsorption Ratio, Effective Salinity and Potential Salinity of the groundwater.

3.3. The Spatial Distribution of the Groundwater Quality for Agricultural Use

The chloride map, due to having the best indicators of spatial analysis, was selected to identify the areas with different groundwater qualities. This map has three zones with no restriction, low to moderate restriction, and severe restriction for agricultural use, according to which the Miandoab Plain was classified into three zones: the east, center, and west of the plain.

3.3.1. Zone (1); East Plain

According to the zoning maps (Figs. 6 and 7) of the east side of the plain, it was found that the EC and ES values are indicators of medium water quality, the PS values with two ranges represent good and medium quality, and SAR shows excellent quality (Table 9). In this zone, the concentrations of sodium and bicarbonate are low, indicating no restriction and low to moderate restriction, respectively, in terms of water toxicity. The chloride content in both ranges indicates low concentration, and thus low toxicity, representing no restriction and low to moderate restriction (Table 9). Therefore, the water quality in the east side of the plain is in good to medium condition and is recommended for agricultural use.

3.3.2. Zone (2); West Plain

The zoning maps (Figs. 6 and 7) of the west parts of the plain demonstrate low water quality based on the values of EC, ES, and PS (Table 9). Owing to the high values of these three parameters, the water quality cannot be recommended (Richards, 1954; Palacios and Aceves, 1970). In this zone, the concentrations of sodium and chloride are very high, resulting in severe toxicity. The bicarbonate content with two ranges has a toxicity level of higher than 3.5 mmol L^{-1}, indicating moderate and severe restriction. However, in the west of the plain, only in terms

of SAR the water quality is good and excellent with no restriction (Table 9). In general, the results show that in this zone, due to the high salinity and the high concentrations of chloride, bicarbonate, and sodium, the toxicity hazard to crops is severe. Therefore, the water in the west plain is of low quality and is not recommended for agricultural use. This can be a warning sign of the extreme exploitation of groundwater.

3.3.3. Zone (3); Central Plain

The zoning maps (Figs. 6 and 7) of the central parts of the plain show medium and unrecommendable water quality based on EC and ES values with two ranges. The SAR values indicate both excellent and good quality, and the PS values represent medium quality. The sodium concentration is in two ranges with no restriction and severe restriction. The chloride concentration is almost low, indicating low to medium toxicity. The bicarbonate concentration is also in two ranges with toxicity of higher than 3.5 mmol L^{-1}, representing moderate to severe restriction. Overall, in order to use the groundwater for agricultural purposes in the central parts of the plain, in addition to monitoring the soil salinity, the aquifer in the east and west of the plain should be taken into account and the quality indices and other necessary measures should be applied (Table 9).

Table 9. The zones of the groundwater quality for agricultural use based on the hazards of toxicity, salinity and sodicity.

Zones	Cl^- (mmol L^{-1})	Hco_3^- (mmol L^{-1})	Na^+ (mmol L^{-1})	ES (mmol L^{-1})	PS (mmol L^{-1})	SAR (mmol $L^{-1})^{0.5}$	EC (µmhos Cm^{-1})	Classification Ec+SAR
1; (East Plain)	1.1-3.9=WR 4.1-8.6=S-M	3.5-7=S-M	1.8-8.4=WR	3.75-13.9=M	1.85-2.8=G 3.13-13.25=M	1.34-9.97=E	829.12-2154.12=M	C_3S_1
2; (West Plain)	9.5-54.4=S	3.5-7=S-M 7.8-14.7=S	11.7-46=S	15.5-63.7=NR	17.45-58.75=NR	1.34-9.97=E 10.16-16.74=G	2385.29-7690=NR	C_4S_1, C_4S_2
3; (Centeral Plain)	4.1-8.6=S-M	3.5-7=S-M 7.8-14.7=S	1.8-8.4=WR 11.7-46=S	3.75-13.9=M 15.5-63.7=NR	3.13-13.25=M	1.34-9.97=E 10.16-16.74=G	829.12-2154.12=M 2385.29-7690=NR	C_3S_1, C_3S_2, C_4S_1, C_4S_2

WR=Without Restriction; S–M= Slight to Moderate; M=Medium; S = Severe; G= good; N= Not Recommended; ES = Effective Salinity; PS = Potential Salinity; SAR = Sodium Adsorption Ratio; EC = Electric Conductivity.

According to the zoning maps, chloride shows low to medium toxicity in the aquifer recharge area, which considering the parameters of potential salinity (Eq. 2), this can also be the reason for the medium potential salinity in this area. Similarly, toward the discharge area, with increasing the chloride toxicity, the potential salinity also increases (Figs. 6a and 7d). Since bicarbonate is involved in the calculation of effective salinity (Eqs. 3-6), the bicarbonate toxicity at the entrance compared to the end of the plain can indicate effective salinity in the recharge and drainage areas to some extent (Figs. 6b and 7c).

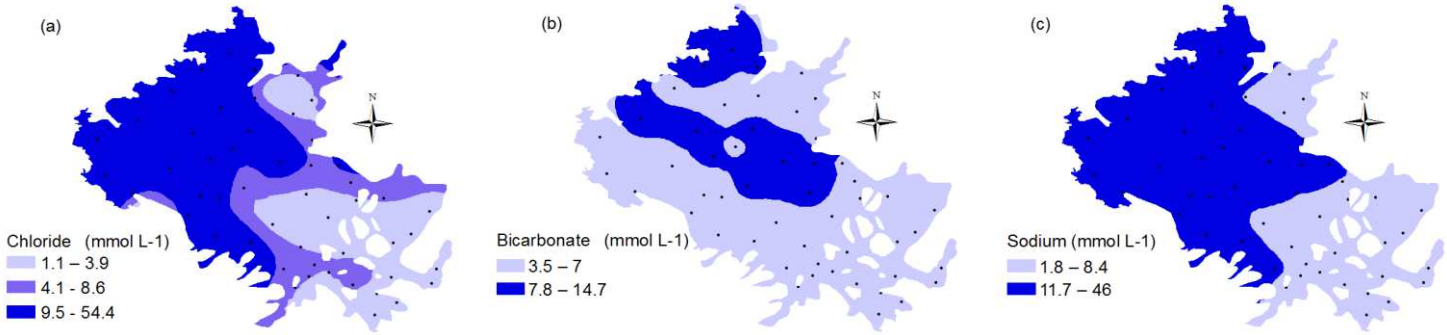

Fig. 6. The zoning maps of the ions contents in the groundwater.

According to the general trend of changes in groundwater, i.e. the Chebotarev sequence (1955), groundwater at the entrance (recharge area) is bicarbonate, which gradually changes to

sulfate in the middle of the plain and finally, to chloride at the end (discharge area). Thus, considering the concepts of effective salinity and potential salinity, the bicarbonate and chloride contents respectively in the recharge and discharge areas (Figs. 6a and 6b), confirm the changes in the effective salinity and potential salinity (Figs. 7c and 7d).

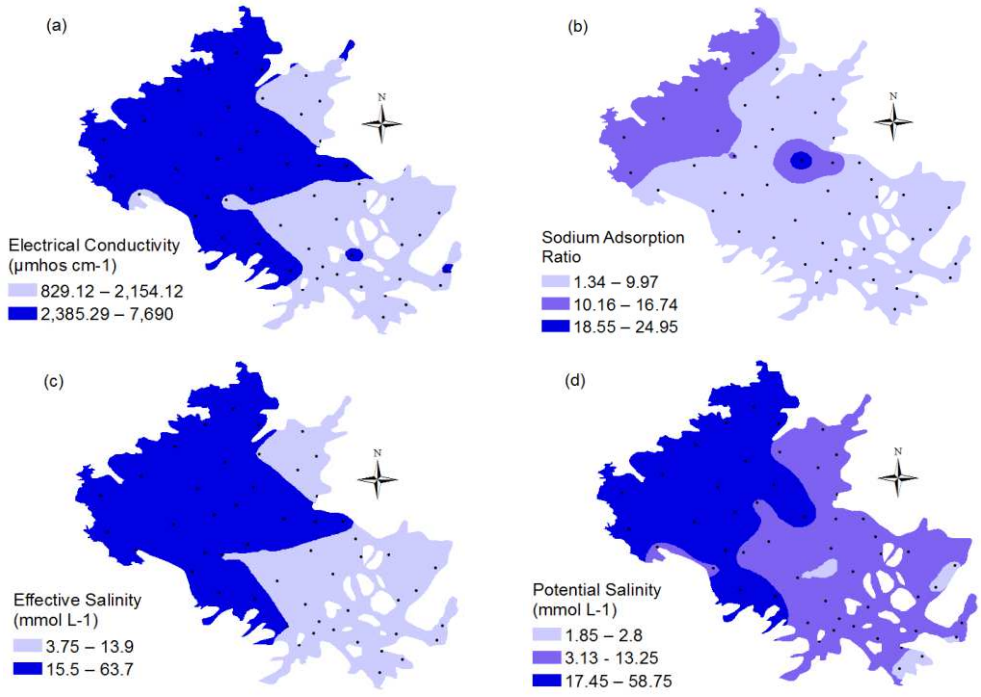

Fig. 7. The zoning maps of Electrical Conductivity, Sodium Adsorption Ratio, Effective Salinity and Potential Salinity in the groundwater.

4. Conclusions

The spatial and temporal changes in the groundwater quality in the Miandoab Plain were investigated using the data set of 2002-2018 from 51 wells. The quality parameters were normalized and then analyzed using the Kolmogorov-Smirnov test at a significance level of 5% in Spss22. The presence or absence of a trend in the data was examined using Excel. The geostatistical analyses were performed using GS^+ and the zoning maps of the groundwater salinity hazard were prepared using ArcGIS. The chloride semi-variogram obtained by the Gaussian model displayed the best spatial distribution of EC, ES, PS, and SAR as well as Hco_3^- and Na^+ in the plain.

The zoning maps of EC, ES, PS, SAR, Cl^-, Hco_3^-, and Na^+ showed that the groundwater salinity and toxicity increase from the recharge areas (the north-east, east, south-east, and south) toward the discharge areas (the north-west, west, and partly south-west) of the plain. It can be concluded that salinity is higher in the west of the plain, which can partly be due to the existence of Lake Urmia in the west side. Since the aquifer is discharged into Lake Urmia, which is in turn the cause of the salinity, with the increase of groundwater abstraction from the plain, the way for the saline water to flow from the lake to the aquifer is facilitated, which in turn, intensifies the salinity. Therefore, the recharge area (east) is the low-risk side, and the discharge area (west) is the high-risk side of the plain.

According to the zoning maps (Figs. 6 and 7) and zoning table (Table 9), EC and ES were found to be highly consistent with each other, but the compatibility between PS and Cl^- was even more.

To summarize, in the west of the Miandoab Plain, the groundwater quality cannot be recommended for agricultural uses. In the central part, if there is necessity to use the groundwater, the quality should constantly be monitored by applying appropriate measures. However, in the east of the plain, the quality is good to medium and is recommended for agricultural uses.

Conflict of Interest:

Authors certify that there is no conflict of interest in this research.

References

1) Abbasi, E. and Khosravi, Y. (2015). Spatial Analysis of Environmental Data Using Geostatistics. Azarkelk Publication. (In Persian).
2) Ayers, R.S. and Wescott, D.W. (1994). Water quality for agriculture. FAO Irrigation and Drainage Paper 29. Rev. 1. Rome, Italy. 97 p.
3) Bagheri, R. and Mohammadi, S. (2009). Comparing different interpolation methods to investigate the spatial changes in the water-table of Kerman Plain. The 1st National Conference on Groundwater, Behbahan, Iran. (In Persian).
4) Chebotarev, I.I. (1955). Metamorphism of natural waters in the crust of weathering. Geochimica et. Cosmochimica Acta, 8, pp 22 - 48, 137 - 170, 198 -. 212. COBB, P.M., MCELWEE, C.D.
5) Delgado, C., Pacheco, J., Cabrera, A., Batllori, C. E., Orellana, R. and Bautista, F. (2010). Quality of groundwater for irrigation in tropical karst environment: The case of Yucatan, Mexico: Agricultural Water Management; 97(10): 1423-1433.
6) ElKashouty, M. (2019). Groundwater quality distribution by geostatistical investigation (GIS), Nile Delta, Northern Egypt: Journal of Environmental Chemistry and Ecotoxicology: Vol. 11(1), pp. 1-21.
7) Elubid, A. B., Tao Huang, T., Ekhlas, H., Ahmed, E. H., Zhao, J., Elhag, K. M., Abbass, W. & Babiker, M. M. (2019). Geospatial distributions of groundwater quality in Gedaref State using geographic information system (GIS) and drinking water quality index (DWQI). Int. J. Environ. Res. Public Health 16 (5), 2–20.
8) Emami, S., Choopan, Y. and Parsa, J. (2018). Modelling the groundwater level of the Miandoab Plain using artificial neural network method and election and genetic algorithms. Iranian Journal Echohydrology, 5 (4): 1175-1189. (In Persian)
9) Gharbia, A.S., Gharbia, S.S., Abushbak, T., Wafi, H., Aish, A., Zelenakova, M. and Pilla, F. (2016). Groundwater Quality Evaluation Using GIS Based Geostatistical Algorithms. Journal of Geoscience and Environment Protection; 4: 89-103.
10) Ghasemi-Ziarani, A., faryadi, Sh., and Shaykh Kazemi, Sh. (2006). The pollution of the Karaj dam basin by using GIS software, the first environmental engineering conference, Tehran University, Faculty of Engineering.
11) GS+ (Gamma Design Software). (2006). Geostatistics for the Environmental Sciences. GS+ User's Guide. Version 7. Plainwell, MI, USA.
12) Habibi, A. (2016). Practical Application of SPSS Software. 4th Edition, Pars Modir Electronic Publication. (In Persian)

13) Hamzah, Z., Aris, A. Z., Ramli, M. F., Juahir, H. and Narany, T. S. (2017). Groundwater quality assessment using integrated geochemical methods, multivariate statistical analysis, and geostatistical technique in shallow coastal aquifer of Terengganu, Malaysia. Arabian Journal of Geosciences; 10(2):49.
14) Hernandez-Stefanoni, J.L. and Ponce-Hernandez, R. (2006). Mapping the spatial variability of plant diversity in a tropical forest: comparison of spatial interpolation methods. Environ. Monit. Assess. 117, 307–334.
15) Honarbakhsh, A., Azma, A., Nikseresht, F., Mousazadeh, M., Eftekhari, M. and Ostovari, Y. (2019). Hydro-chemical assessment and GIS-mapping of groundwater quality parameters in semi-arid regions. Journal of Water Supply: Research and Technology- AQUA.
16) Isaaks, E.H. and Srivastava, R.M. (1989). An Introduction to Applied Geostatistics. Oxford Univer. Press, New York, USA.
17) Jeon, Ch., Raza, M., Lee, J.Y., Kim, H., Kim Ch.S., Kim, B., Kim, J. W., Kim, R. K. and Lee, S. W. (2020). Countrywide Groundwater Quality Trend and Suitability for Use in Key Sectors of Korea: Water: MDPI.
18) Jonubi, R., Rezaverdinejad, V., Behmanesh, J. and Abbaspour, K. (2018). Investigation of quantitative changes in the groundwater table of the Miandoab Plain affected by surface and groundwater resources management using the MODFLOW-NWT mathematical model. Iranian Journal of Soil and Water Research, 49 (2): 467-481. (In Persian)
19) Kaur, T. Bhardwaj, R. and Arora, S. (2017) .Assessment of groundwater quality for drinking and irrigation purposes using hydrochemical studies in Malwa region, southwestern part of Punjab, India. Applied Water Science. 7(6), 3301-3316.
20) Kirda, C. (1997). Assessment of irrigation water quality. CIHEAM Options Mediterranean's: 367-377.
21) Kresic, N. (1997). Hydrogeology and Groundwater Modeling. Lewis Publishers.
22) Maas, E. V. and Grattan, S. R. (1999). Crop yield as affected by salinity. In: Skaggs R. W. and van Schilfgaarde J. (eds.), Agricultural Drainage Agron. Monograph. 38. ASA, CSSA, SSSA, Madison, WI. pp. 55-107.
23) Maas, E. V. and Hoffman, G. J. (1977). Crop salt tolerance –current assessment. J. Irrig. Drainage Div, ASCE. 103(2):115-134.
24) Maroufpoor, S., Fakheri-Fard, A. and Shiri, J. (2019). Study of the spatial distribution of groundwater quality using soft computing and geostatistical models. ISH Journal of Hydraulic Engineering; 25(2):232-8.
25) Nazarizadeh, F., Ershadian, B., ZandVakili, K., and Nouriemamzade'i, M. (2006). Investigating the variations in groundwater quality in Balarood plain in Khuzestan province.
26) Noroozi-Qushbulaq, H., Asghari-Moghaddam, A. and Hateftabar, S. (2019). Evaluation of the vulnerability of the Miandoab Plain to nitrate using the genetic algorithm. Ecology, 45 (2): 301-315. (In Persian).
27) Palacios, V.O. and Aceves, N.E. (1970). Instructivos para el muestreo, registro de datos e interpretacion de la calidad del agua para riego agricola. Colegio de Postgraduados, Chapingo, Mexico.

28) Rafi Sharifabad, J., Nohegar, A., Zehtabian, Gh.R. and Gholami, H. (2017). Tracking temporal and spatial changes in underground water quality for potable and agricultural purpose (Case study: Yazd, Ardakan Plain). Desert management, 5 (9): 107-119. (In Persian).
29) Richards, L.A. (1954). Diagnosis and Improvement of Saline and Alkali Soils. Handbook, USDA 60. Washington DC, USA.
30) Safiur Rahman, M., Saha, N., Towfiqul Islam, A. R. M., Shen, Sh. and Bodrud-Doza, Md. (2017). Evaluation of Water Quality for Sustainable Agriculture in Bangladesh: Water Air Soil Pollut; 228-385.
31) Shaabani M. (2009). Determination of the most suitable geostatistical method for mapping of groundwater pH and TDS (a case study: Arsanjan plain). Journal of Water Engineering. 1:47-59.
32) Saleh, A., Al-Ruwaih, F. and Shehata, M. (1999). Hydrogeochemical processes operating within the main aquifers of Kuwait. Journl of Arid Environments. 42,195-209.
33) Sanches, F. (2001). Mapping groundwater quality variables using PCA and Geostatistics: a case study of Bajo Andarax, southern Spain. Hydrologiques. 46(2):227-242.
34) Subramani, T., Elango, L. and Damodarasamy, S.R. (2005). Groundwater quality and its suitability for drinking and agricultural use in Chithar River Basin, Tamil Nadu, India. Journal of Environmental Geology. 47, 1099-1110.
35) Taheri Tizro, A., and Mohamadi, M. (2019). Geostatistical Approach for Groundwater Quality Evaluation in Zarin Abad Plain, Iran: Iranian Journal of Health Sciences; 7(3): 9-20.
36) Verma, P., Singh, P. K., Sinha, R. R. and Tiwari, A. K. (2020). Assessment of groundwater quality status by using water quality index (WQI) and geographic information system (GIS) approaches: a case study of the Bokaro district, India. Applied Water Science (2020) 10:27.
37) Webster, R., and Oliver, M.A. (1990). Statistical Methods in Soil and Land Resource Surrey. Oxford University Press, New York, USA.
38) Wilcox, L. V. (1955). Classification and Use of Irrigation Waters. US DA, Circular 969, Washington.